Encapsulated Drop Breakup in Shear Flow

K. A. Smith* and J. M. Ottino
Department of Chemical and Biological Engineering, Northwestern University, Evanston, Illinois 60208, USA
M. Olvera de la Cruz
Department of Materials Science and Engineering, Northwestern University, Evanston, Illinois 60208, USA
(Received 24 April 2004; published 8 November 2004)

We investigate the deformation and breakup in shear flow of an encapsulated drop in which both the core and shell are Newtonian fluids. The equations of motion are solved numerically using a level set method to track interface motion. We consider the case of a drop stretched to a given length in constant shear and then allowed to relax. A range of morphologies is produced, and novel kinematics occur, due to the interaction of the core and outer interfaces. A phase diagram is presented to describe the morphologies produced over a range of capillary numbers and core interfacial tensions.

DOI: 10.1103/PhysRevLett.93.204501 PACS numbers: 47.85.Dh, 47.55.Dz

Encapsulated drops are common morphologies in incompatible ternary fluids. They often occur in the late stages of phase separation [1–4] and have been expressly created by several new methods [5–10]. Important applications are found in materials processing [11], and targeted drug delivery [12–14], but also as models of more complex systems including blood cells [15] and compatibilizers or emulsifiers [16,17].

The dynamics of encapsulated drops in imposed flow fields is important in industrial settings such as the processing of multicomponent immiscible blends, as well as in cell screening tests. A growing range of microfluidic applications is driving the field [18]; however most of the current work is empirical and many theoretical questions remain open. Simple single-phase drops deform and break upon relaxation via well studied mechanisms [19]. The deformation and relaxation of encapsulated droplets are more complex and can lead to different drop topologies depending on flow conditions. This case is largely unexplored—there are no systematic experimental studies and a only a few limiting cases have been addressed theoretically.

In this Letter we present numerical results for an encapsulated drop in shear flow which show new types of behavior during deformation and breakup. Previous studies [15,20,21] have analyzed deformation in extensional flow, which tends to stretch the shell while compressing the core. Here we show that shear flow deforms the core in tandem with the outer drop and that new behaviors emerge that have no parallel for simple drops.

To study drop dynamics numerically we use a level set representation of the interface [1,22–26] and solve the Navier-Stokes equation:

$$\frac{\partial \mathbf{u}}{\partial t} = -\nabla p - \mathbf{u}\cdot\nabla\mathbf{u} + (1/Re)\nabla^2\mathbf{u} - \mathbf{F} \qquad (1)$$

with $\nabla\cdot\mathbf{u} = 0$. Each interface Γ_i is defined as the zero level set of the function $\phi_i(\mathbf{x}, t)$ and the motion of the interfaces is given by

$$\frac{\partial \phi_i}{\partial t} = -\mathbf{u}\cdot\nabla\phi_i. \qquad (2)$$

Box size is $0 \le x \le 1$; $0 \le y \le 1/2$; and $0 \le z \le 1$ with drop radius $a = 1/8$ and core radius $a_{\text{core}} = a/2$. The drop and the core are concentric and lie at the box center. Moving wall boundaries in the z-direction induce a shear flow $\mathbf{u} = (\dot{\gamma}z, 0, 0)$ where $\dot{\gamma}$ is the shear rate. Other boundaries are periodic. Simulations are done at $\text{Re} = 1/16$, well within the Stokes regime. Densities and viscosities of all phases are equal. The flow strength is defined by a capillary number $\text{Ca} = \mu\dot{\gamma}a/\sigma$ where μ is viscosity, and σ is the drop/outer fluid interfacial tension. The core has an interfacial tension σ_{core} and we define $\kappa \equiv \sigma_{\text{core}}/\sigma$.

To test the method we have measured the deformation of a simple drop as a function of Ca. The results (not shown here) are in quantitative agreement with previous numerical and experimental measurements [27–29], up to the onset of instability at $\text{Ca}_{\text{crit}} = 0.44$. The code also reproduces well known drop breakup mechanisms [19]. At $\text{Ca} \approx Ca_{\text{crit}}$ the drop develops a neck and pinches off before it is highly elongated. At higher Ca drops break up by end pinching and capillary instability.

To show the evolution of the core in detail we first examine a high resolution case ($\Delta x = \Delta y = \Delta z = 1/128$) with low shear, $\text{Ca} = 0.55$ and a weak core, $\kappa = 0.25$ in Fig. 1. (All further results are for $\Delta x = \Delta y = \Delta z = 1/64$. Similar behavior is observed at this resolution.) The drop is sheared until it reaches a half length $L_{\text{outer}} = 3.5a$ and then allowed to relax.

The core evolution does not resemble any type of simple drop behavior in linear flow. In the early stages of elongation both the core and the drop are ellipsoidal and a circulating flow develops inside the drop. However as the drop becomes longer it develops an inflection at its center. At this point the flow in the drop interior changes

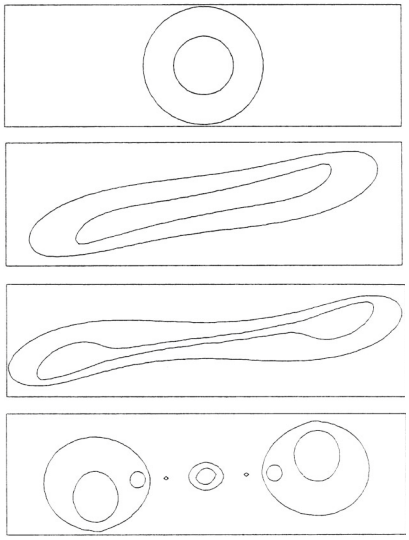

FIG. 1. Time sequence of the deformation of a drop under shear with Ca = 0.55, $\kappa = 0.25$ and subsequent relaxation. Drop radius is $a = 1/8$ and grid resolution is $\Delta x = 1/128$. Shear is turned off when the drop length is 3.5 times its original radius (third image). Images are at time = 0, 10, 14, 20.

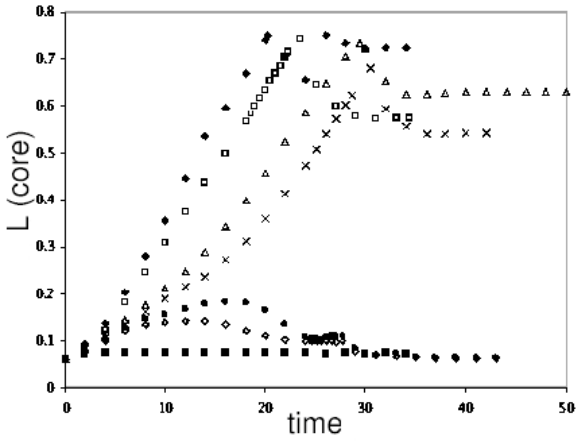

FIG. 2. Time evolution of core length at Ca = 0.55 for $\kappa = 0$ (◆), 0.1 (□), 0.25 (△), 0.3(x), 0.35 (●), 0.4 (◇), and 2 (■). The outer drop is stretched to $L_{\text{outer}} = 0.75$.

and there is a circulating flow in each half of the outer drop. Fluid near the center of the drop is driven to either end, causing the waist to neck down. There is no flow across the center of the drop, so that a fluid element in one half of the drop remains in that half. This has a noticeable effect on the core. The core experiences a large degree of stretching at the drop center while in the drop ends it is able to relax. Thus the core forms bulbous ends connected by a thin thread. This behavior occurs while the drop itself has not undergone significant necking. Thus the evolution of the core is quite different from the evolution of the outer drop, which is stretched by simple shear flow.

Consider now the role of the core strength κ in weak shear (Ca = 0.55). The evolution of core half length L_{core} is shown in Fig. 2 for several values of κ. All results follow a standard protocol in which the drop is stretched in a constant shear flow until $L_{\text{outer}} = 6a = 0.75$, after which the shear is turned off and the drop is allowed to relax. In each case L_{outer} increases steadily under shear. When the shear is turned off L_{outer} decreases (as the drop retracts under interfacial tension) until the drop breaks up into three or more daughter droplets. After this L_{outer} remains constant. Final states are characterized by the number of daughter drops formed and whether each one is a simple or encapsulated drop. Results for various κ are summarized in a "phase diagram" in Fig. 4, which also includes results at several Ca. For $\kappa \leq 0.3$ a series of encapsulated daughter drops are formed. For $\kappa = 0.35$ the core does not break up and the end result is an encapsulated drop surrounded by two single-phase drops. As κ is increased from 0 to 0.3 the drop stretches more slowly but in each case the core is stretched to nearly the same length as the drop. However at $\kappa = 0.35$ the core reaches a maximum length and retracts to a steady shape *while the drop is under shear*. This retraction is in part due to the outer interface. There appears to be a critical length at which the core is no longer able to continue stretching and is driven to retract.

At a high shear rate (Ca = 2) the picture is quite different. As κ is increased from 0 to 1 the core deformation decreases steadily (see Fig. 3). However, even at the highest κ we see a continuous stretching of the core. There is no indication of a sudden change in behavior as seen in weak shear.

The relaxation process is also different at high shear. It has been shown [30] that drops deformed at high shear have tapered ends and are thus slower to undergo end pinching. This is the case for $\kappa \leq 0.2$, where the drop relaxes back to its initial shape for Ca = 2 (Fig. 4). At $\kappa \geq 0.25$ the core relaxes rapidly to a sphere, creating a bulge at the drop center which incites end pinching.

These results highlight an important difference between weak and strong shear. At high Ca the core can be stretched at most at the same rate as the drop so that $L_{\text{core}} \approx L_{\text{outer}}/2$. At low Ca there is a significant amount of circulation in the drop during deformation. For low κ this internal flow stretches the core, towards the ends of the drop, so that $L_{\text{core}} \approx L_{\text{outer}}$. Above a critical κ the core retracts and remains at a constant L_{core}. Thus weak shear is more effective at stretching the core at low κ while strong shear is more effective at high κ.

A study over the full range of Ca and κ reveals a variety of topologically distinct outcomes (Fig. 4). In some instances the drop relaxes without breaking up. In other cases the drop breaks into two or more encapsulated drops. Finally the drop may form a single encapsulated drop surrounded by single-phase drops.

Many of the results can be explained in terms of predictable limiting behaviors, such as an undeformed

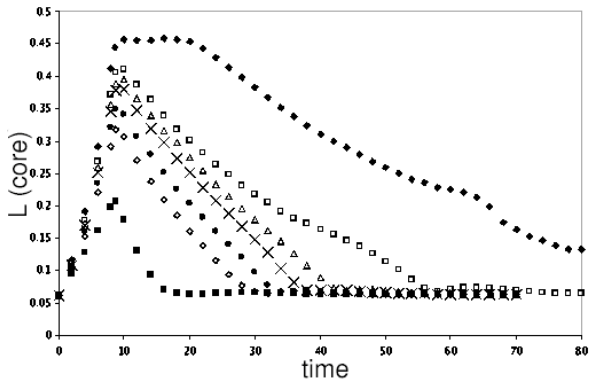

FIG. 3. Time evolution of core length at Ca = 2 for $\kappa = 0$ (◆), 0.2 (□), 0.25 (△), 0.3 (x), 0.4 (●), 0.5 (◇) and 1 (■).

core at large κ or affine deformation at high Ca. We can identify three such limits: (i) At small κ and low Ca the drop breaks into a series of encapsulated daughter drops through end pinching and capillary instability. (ii) At large κ the core undergoes little deformation, forming a bulge which causes the outer drop ends to pinch off. (iii) At small κ and high Ca the drop relaxes back to a sphere. Of greater interest are the unique behaviors at intermediate parameter values which are driven by the interplay between various effects.

In case (i) the core is largely passive and breaks up due to instabilities of the outer interface. With increasing κ core effects become more important. For Ca = 0.69 the final morphology at $\kappa = 0.25$ is nearly identical to that of $\kappa = 0$, with three drops of nearly equal size. However for $\kappa = 0.3$ (Fig. 5) the core effects the final morphology. At the start of relaxation the drop ends become bulbous and develop necks. In this case the ends of the core lie in the

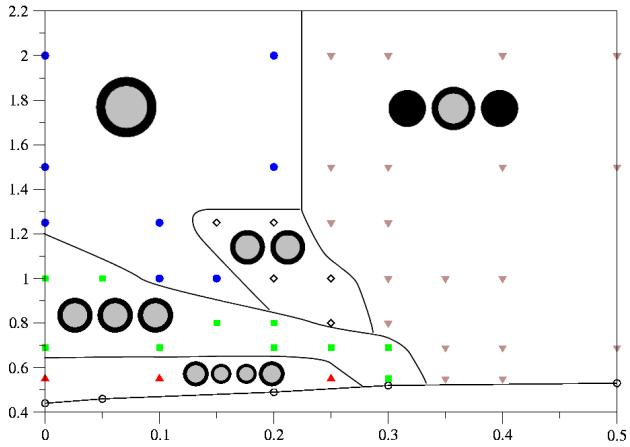

FIG. 4 (color online). Phase diagram representing the dependence of final drop morphology on Ca and κ for a total of 50 computations. Points represented by identical symbols indicate cases which reached topologically equivalent final states, as illustrated in each region. Boundaries are drawn as a guide to the eye. The lowest curve contains measured values of Ca_{crit} as a function of κ.

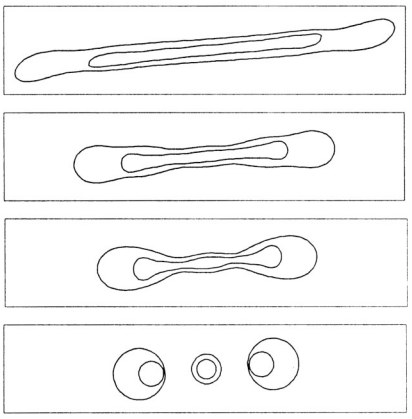

FIG. 5. Time sequence of drop relaxation after shear is turned off. Drop was first stretched to 6 times its original radius with Ca = 0.69 and $\kappa = 0.3$. Original radius is $a = 1/8$ and grid resolution is $\Delta x = 1/64$. Images are at time =16, 28, 34, 41.

region where the outer drop forms necks and so they interfere with end pinching. As the drop relaxes further two necks eventually appear close to the center of the drop. The consequence of this delay is that the central daughter drop is much smaller than the others and all three drops lie closer together than for lower κ.

In other situations the presence of the core can prevent breakup altogether. At Ca = 0.1 a drop with a weak core undergoes end pinching. However at $\kappa = 0.1$ and $\kappa = 0.15$ the drop is stabilized against breakup (see Fig. 6). This stability is not due to end tapering such as that observed at high Ca. Instead the core forms bulbous ends which inhibit end pinching by the outer interface. At the same time the shape of the core does not allow the drop to form a neck at the center so that eventually the entire drop relaxes to its initial shape.

Finally a distinct morphology, two encapsulated drops, is produced at intermediate values of Ca and κ. A repre-

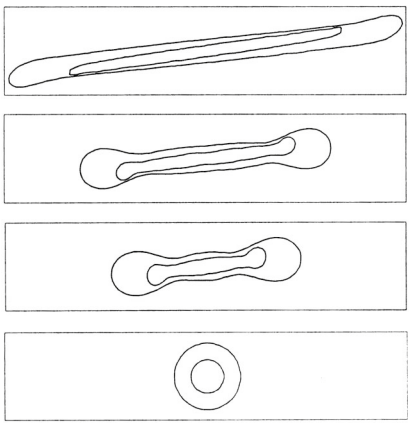

FIG. 6. Time sequence of drop relaxation after shear is turned off. Drop was first stretched to 6 times its original radius with Ca = 1 and $\kappa = 0.15$. Original radius is $a = 1/8$ and grid resolution is $\Delta x = 1/64$. Images are at time =12, 30, 42, 52.

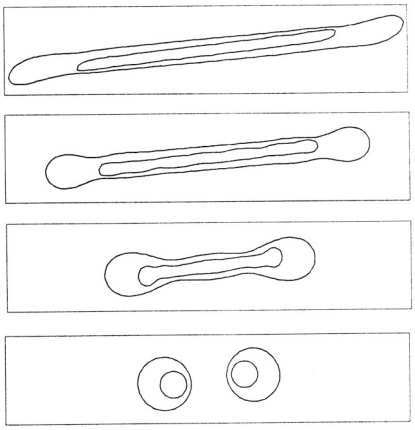

FIG. 7. Time sequence of drop relaxation after shear is turned off. Drop was first stretched to 6 times its original radius with Ca = 0.8 and $\kappa = 0.25$. Original radius is $a = 1/8$ and grid resolution is $\Delta x = 1/64$. Images are at time =13, 23, 31, 43.

sentative case is Ca = 0.8, $\kappa = 0.25$ (Fig. 7). When the core is either weaker ($\kappa = 0.2$) or stronger ($\kappa = 0.3$) the drop undergoes end pinching. In the former case the core breaks up while in the latter case it does not, but in neither case does it interfere with end pinching. However for $\kappa = 0.25$ the core again inhibits end pinching. As the drop retracts further it develops a single neck at the center where both the core and the outer drop pinch off. This behavior occurs over an extended region of the phase diagram.

It is well known that the behavior of sheared drops depends on the ratio of shear forces to interfacial tension. For encapsulated drops we have added a third parameter, the core interfacial tension, and find that this introduces greater variety in the dynamics of both deformation and relaxation. These results show that drops with differing properties (such as κ) can behave similarly under certain flow conditions but quite differently under others. The evolution of drop size and topology under shear is strongly affected [31]. We also expect shear induced coalescence of drops [32] to be affected.

Studies of dynamics of breakup of simple drops have long involved a healthy interplay between experiment and computation. It is clear that experimental studies of the dynamics of compound drops are now needed to advance knowledge in this area.

This work was supported by IGERT-NSF grant no. 9987577 and by NSF grant no. DMR-0109610.

*Current address: LPMCN, Universite Claude Bernard & CNRS, 69622 Villeurbanne, France
Electronic address: ksmith@lpmcn.univ-lyon1.fr

[1] K. A. Smith, F. J. Solis, L. Tao, K. Thornton, and M. O. de la Cruz, Phys. Rev. Lett. **84**, 91 (2000).
[2] S. Walheim, M. Ramstein, and U. Steiner, Langmuir **15**, 4828 (1999).
[3] C. Huang, M. O. de la Cruz, and B.W. Swift, Macromolecules **28**, 7996 (1995).
[4] C. Huang and M. O. de la Cruz, Phys. Rev. E **53**, 812 (1996).
[5] R. Gref, Y. Minamitake, M.T. Peracchia, V. Trubetskoy, V. Torchilin, and R. Langer, Science **263**, 1600 (1994).
[6] R. A. Jain, Biomaterials **21**, 2475 (2000).
[7] J. R. Lister, J. Fluid Mech. **198**, 231 (1989).
[8] I. Cohen, H. Li, J. L. Hougland, M. Mrksich, and S. R. Nagel, Science **292**, 265 (2001).
[9] A. M. Gãnan-Calvo, Phys. Rev. Lett. **80**, 285 (1998).
[10] I. G. Loscertales, A. Barrero, I. Guerrero, R. Cortijo, M. Marquez, and A. M. Gãnan-Calvo, Science **295**, 1695 (2002).
[11] Y. H. Lee, C. A. Kim, W. H. Jang, H. J. Choi, and M. S. Jhon, Polymer **42**, 8277 (2001).
[12] E. Mathiowitz, J. S. Jacob, Y. S. Jong, G. P. Carino, D. E. Chickering, P. Chaturvedi, C. A. Santos, K. Vijayaraghavan, S. Montgomery, M. Bassett *et al.*, Nature (London) **386**, 410 (1997).
[13] R. T. Bartus, M. A. Tracy, D. F. Emerich, and S. E. Zale, Science **281**, 1161 (1998).
[14] R. Langer, Nature (London) Suppl. **392**, 5 (1998).
[15] H.-C. Kan, H. S. Udaykumar, W. Shyy, and R. Tran-Son-Tay, Phys. Fluids **10**, 760 (1998).
[16] S. T. Milner and H.W. Xi, J. Rheol. **40**, 663 (1996).
[17] J. F. Wang, H. D. Zhang, F. Qiu, Z. G. Wang, and Y. L. Yang, J. Chem. Phys. **118**, 8997 (2003).
[18] See for instance http://www.jintanworld.com.
[19] H. A. Stone, Annu. Rev. Fluid Mech. **26**, 65 (1994).
[20] H. A. Stone and L. G. Leal, J. Fluid Mech. **211**, 123 (1990).
[21] J.W. Ha and S. M. Yang, Phys. Fluids **11**, 1029 (1999).
[22] S. Osher and J. Sethian, J. Comput. Phys. **79**, 12 (1988).
[23] M. Sussman, P. Smereka, and S. Osher, J. Comput. Phys. **114**, 146 (1994).
[24] Y. Chang, T. Hou, B. Merriman, and S. Osher, J. Comput. Phys. **124**, 449 (1996).
[25] K. A. Smith, F. J. Solis, and D. L. Chopp, Interface Free Bound. **4**, 263 (2002).
[26] K. A. Smith, J. M. Ottino, and M. O. de la Cruz, Phys. Rev. E **69**, 046302 (2004).
[27] G. I. Taylor, Proc. R. Soc. London A **146**, 501 (1934).
[28] F. D. Rumscheidt and S. G. Mason, J. Colloid Sci. **16**, 238 (1961).
[29] J. Li, Y. Y. Renardy, and M. Renardy, Phys. Fluids **12**, 269 (2000).
[30] J.W. Ha and L. G. Leal, Phys. Fluids **13**, 1568 (2001).
[31] B. E. Burkhart, P.V. Gopalkrishnan, S. D. Hudson, A. M. Jamieson, M. A. Rother, and R. H. Davis, Phys. Rev. Lett. **87**, 098304 (2001).
[32] A. Nandi, A. Mehra, and D.V. Khakhar, Phys. Rev. Lett. **83**, 2461 (1999).